THE ANALYST
FULL PAPER
www.rsc.org/analyst

Viscoelasticity in the diffuse electric double layer†

Roberto Etchenique*[a] and Thomas Buhse[b]

[a] *INQUIMAE DQIAyQF Facultad de Ciencias Exactas y Naturales, Pab. 2, Universidad de Buenos Aires, Ciudad Universitaria, CP 1428 Buenos Aires, Argentina. E-mail: rober@q1.fcen.uba.ar; Fax: +54 11 4576-3341; Tel: +54 11 4576-3358*
[b] *Centro de Investigaciones Químicas, Universidad Autónoma del Estado de Morelos, Av. Universidad N 1001, Col. Chamilpa, 62210 Cuernavaca, Mor, México*

Received 1st July 2002, Accepted 19th August 2002
First published as an Advance Article on the web 29th August 2002

The electroacoustical impedance of the quartz crystal microbalance (QCM) in contact with aqueous electrolyte solutions was measured using the transfer function method in a flow injection system . Measurements of both components of the impedance of the QCM, the resistance *R* and the inductive reactance *XL*, have been performed for modified and bare gold and silver surfaces and for different concentrations of several aqueous electrolyte solutions. For the experimental concentration range of 0–50 mM, unexpectedly the QCM impedance does not follow the Kanazawa equation, as is usual for bulk newtonian liquids. This behavior indicates the presence of a nanometric sized viscoelastic layer between the piezoelectric crystal and the bulk electrolyte solution. This layer can only be identified as the Gouy–Chapman diffuse double layer (DDL). Its elasticity and viscosity have been estimated by the measurement of *R* and *XL*. The viscoelasticity of the DDL appears to be independent of the chemical nature of the surface and of the solution viscosity but strongly dependent on the surface charge, the bulk electrolyte concentration and the dielectric constant of the solvent.

1. Introduction

The diffuse electric double layer in the interface between an electrode and a liquid electrolyte has been profusely investigated due to its crucial role in interfacial systems. Measurements of the related phenomena, *i.e.* double layer capacitance,[1] electrocapillary curves,[2] *etc.* have been performed routinely for many electrode–electrolyte combinations. The Gouy–Chapman diffuse double layer (DDL) and its properties have also been studied by simulations.[3] Although considerable advances have been made in the understanding of double layer structures, direct measurements of their mechanical properties are limited. In 1996, Bard *et al.*[4] measured for the first time the forces between the DDL and a charged sphere in a nanometric scale using atomic force microscopy.

Quartz crystal microbalance (QCM) impedance analysis has been widely used to measure the viscoelastic properties of materials such as polymers,[5] molecular composites[6] or gels.[7] In the last years, several models and procedures have been established in order to measure rheological properties of thin films.[8] In a previous short Communication[9] we have shown that the presence of electrolytes introduces a significant error in the analytical determination of adsorbed species using QCM even by means of full impedance analysis. We attributed this anomalous behaviour to the changes in the rheological properties of the DDL. A similar effect had been reported,[10,11] but only in the cases when parallel resonance is measured. Afterwards, different electrode configurations were used to determine the origin of this effect.[12] In this work, we complete our analysis, using for the first time QCM impedance analysis in order to attempt direct determination of high frequency rheological properties of the DDL.

† Electronic supplementary information (ESI) available: QCM impedance measurements. See http://www.rsc.org/suppdata/an/b2/b206305k/

2. Quartz crystal impedance analysis

The mechanical properties of a quartz resonator can be described in terms of an electrical equivalent circuit. The most widely used is the Butterworth–Van Dyke model, which consists of a motional impedance in parallel with a parasitic capacitance C_0, due to the connections, cables and the quartz itself. The motional impedance consists of a series *RLC* circuit where *R* and *L* are related with the properties of the resonator and also with the layers attached to it. The inductive part L_f of the impedance Z_f is linearly related to the shift in resonant frequency. For rigidly coupled materials, it is also proportional to the change in mass. This linear relationship between the resonant frequency and the mass is the basis of the QCM microgravimetry. The resistive part R_f is related to the broadening of the impedance curve around resonance, and to the energy loss in the film due to friction and viscous coupling. For an homogeneous viscoelastic film covered with a semi-infinite liquid, *R* and *L* follows Martin's equation for bilayers. A more complete explanation is given elsewere.[9]

3. Experimental setup

Polished 14 mm gold and silver coated AT cut quartz crystals (ICM Company Inc. Oklahoma City, USA) were mounted on a 50 μL flow injection QCM, with only one face in contact with the carrier. The operation mode is described in the previous Communication.[9]

The QCM setup and the transfer function method to measure QCM impedance have been described elsewhere.[13] In brief, the measuring circuit consists of an ac voltage divider formed by a quartz resonator impedance *Z* and a measuring capacitor C_m. A sinusoidal signal generated by a computer controlled variable frequency oscillator (VFO) is applied to the input of the

transference voltage divider. Both the input V_i and output V_o were amplified, rectified and measured with a 12 bits A/D board attached to a 586 computer. The BVD equivalent parameters R, L and C_0 were obtained by least square fit of the analytical expression to the measured data.[9,13] Potentials are quoted against saturated calomel electrode (SCE). The chemicals used were of analytical grade.

4. Results and discussion

The dependence of both parameters XL_f and R_f as a function of the concentration of dilute nonelectrolytes is shown in Fig. 1a. For semi-infinite (bulk) solutions one would expect that both R_f and XL_f scale monotonically with the square root of the viscosity.[13] For sucrose solutions, the values of both components are higher than those for ethylene glycol solutions of the same concentration, corresponding to the higher viscosity of the aqueous sugar solutions. In general, for bulk newtonian liquids, the Kanazawa equation holds and $R_f = XL_f$ and for viscoelastic liquids one also observes a linear dependency in which $R_f > XL_f$.[13] In our case, both solutions behave rather as newtonian liquids, as can be seen in Fig. 1b, where the slopes of R_f *vs.* XL_f are close to unity.

In contrast to the former results, Fig. 2 shows the unusual result of a typical experiment by using a dilute electrolyte solution. In this case, the QCM impedance parameters as a function of the electrolyte concentration pass through a maximum. In the inset of Fig. 2, the corresponding parametric plot of the resistance R_f *vs.* the reactance XL_f with the concentration as the variable parameter is given. In this case, the parametric plot of R_f *vs.* XL_f describes an open circle and not a straight line as expected for a semi-infinite liquid. It is known that the response of the QCM to thin layers of variable viscosity and/or elasticity is characterized by a curvature of the R_f *vs.* XL_f plot.[13] For low values of the mechanical modulus G_f, the layer does not move in-phase with the crystal, and the response is characterized by the losses ($R_f \approx XL_f$). For high moduli, the layer is hard enough to move in-phase with the surface, and the impedance is characterized mainly by the inertia, with $XL_f > R_f$.[14,15]

Thus, we conclude that the circular shape of the R_f *vs.* XL_f curve cannot be explained by means of any change in the bulk properties. Therefore, we assume that a thin viscoelastic layer is effectively formed between the quartz crystal and the bulk solution.

(To test reproducibility, six 50 μL aliquotes of aqueous KCl 0.3 M were injected in the carrier feedstream by means of an automatic syringe controlled by the computer. All peaks were equal in shape and size as shown in the Electronic supplementary information (ESI)†).

The flow injection apparatus was also useful to compare the response of the QCM to nonelectrolyte and electrolyte solutions. Fig. 3 shows the first part of an experiment in which aliquotes of glycerol 1 M , sucrose 0.25 M, ethyleneglycol 1.6 M, KCl 0.3 M, $CaCl_2$ 0.2 M and $BaCl_2$ 0.3 M were injected manually to the feedstream. The concentrations were chosen so as to yield similar changes in the QCM impedance. For the nonelectrolyte injections (peaks a, b and c), linear behaviour between R_f and XL_f is observed as expected for semi-infinite liquids. However, when electrolytes are injected (peaks d, e and f) the results are similar to the one in Fig. 2, showing a curvature that can be ascribed to a finite viscoelastic layer close to the quartz. In this case, the R_f *vs.* XL_f plot shows a strong hysteresis, that does not appear in the nonelectrolyte plots.

Fig. 4 shows the complete experiment from which Fig. 3 was extracted. After the first six injections (a to f), at about 1500 s, sucrose was added to the carrier increasing its viscosity, beyond the maximum reached in those peaks. The QCM reflected this change by an increase of about 30 Ω in both R_f and XL_f (bottom figure). After the new baseline is stable, four new injections were performed. The enlargement of this part of the experiment (top figure) shows the injection of glycerol (g), sucrose (h), KCl (i) and NaCl (j). The nonelectrolytes almost do not have any effect in the QCM impedance, since now the relative change in the carrier viscosity is small. On the other hand, the response of the QCM to the electrolytes shows the same behaviour as in Fig.

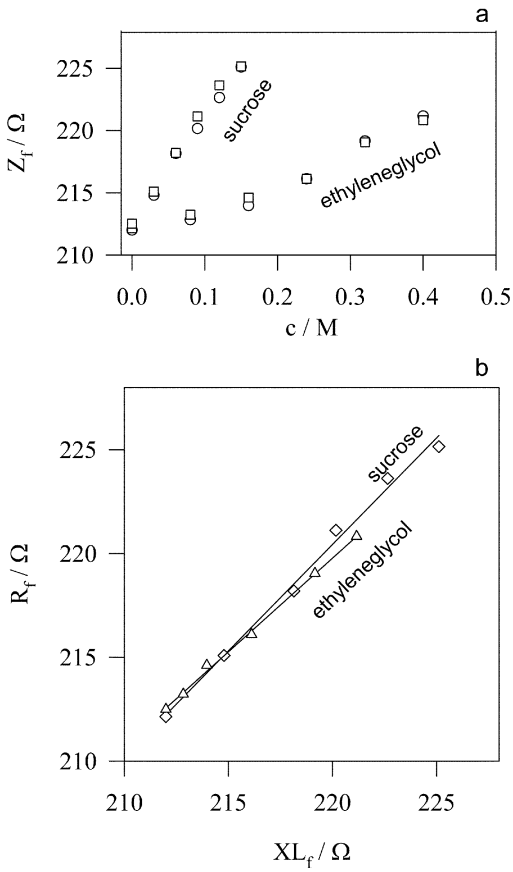

Fig. 1 (a) QCM impedance components R_f (○) and XL_f (□) *vs.* nonelectrolyte concentration. Each point is the mean value of 30 measurements. (b) Parametric plot of R_f *vs.* XL_f, sucrose (△) and ethyleneglycol (◇) concentration are the parameters and increase from bottom to top.

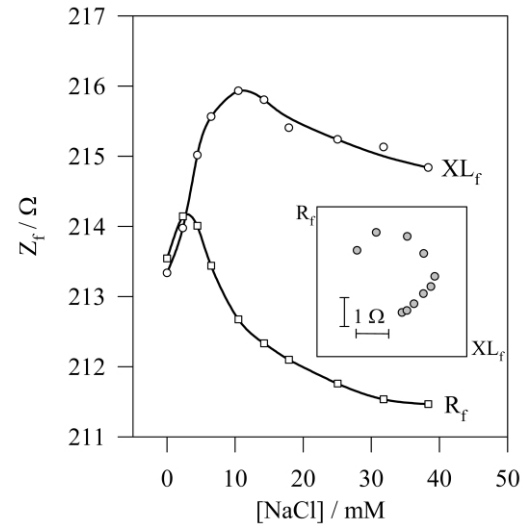

Fig. 2 QCM impedance components R_f and XL_f *vs.* NaCl concentration. Each point is the mean value of 30 measurements. Inset: parametric plot of R_f *vs.* XL_f, [NaCl] is the parameter and increases clockwise.

3, regardless of the change of viscosity. This experiment demonstrates that the effects of nonelectrolytes and electrolytes are different in nature, and even additive in magnitude. In the case of the electrolytes, the parameter that changes is not the viscosity of the bulk, since in this case one would expect the same behaviour showed by nonelectrolytes. Moreover, the viscosity of KCl solutions in a range from 0 to 0.5 M is within 0.5% of that of the pure water and cannot account for the change in the impedance parameters. The QCM response is the same as that for several other electrolytes of higher viscosities (see ESI†). The same response to electrolyte solutions was also observed when silver coated quartz crystals were used.

Since in these cases the solution in contact with the QCM consists exclusively of solvent and electrolyte, the viscoelastic thin layer that the QCM impedance detects can only be identified with the Gouy–Chapman diffuse electric double layer (DDL).

If this was the case, the surface charge should play a role in the described phenomena. In order to determine it, a potentiostatic experiment was performed. By connecting the gold electrode to a fixed potential, its charge can be varied within a certain range. Fig. 5a shows the parametric plots for the QCM impedance measured at −100 mV and −50 mV *vs.* SCE, while varying the concentration from 0 to 6 mM. It can be seen that at a potential of −50 mV, the open circle is smaller than the one correponding to the −100 mV experiment. Fig. 5b shows the diameter of these open circles plotted against the potential between −100 mV and +50 mV. The minimum diameter would be located slightly above −50 mV.

Thus, we can identify the minimum in diameter with the potential of minimum charge (pmc) of our polycrystalline gold; this value is in good agreement with previous work.[4] For a gold monocrystal, it is possible to choose the potential of zero charge (pzc) and to vary it slightly to see the differences in the QCM response. Unfortunately, our gold covered crystals present different crystallographic faces to the solution, and each face has a different pzc. As a consequence, there is never real zero charge on the surface, but only a minimum charge.[19]

The gold electrode was also derivatized with aminoethanethiol and mercaptopropanesulfonate[20] in order to control the charge of the surface, which can be also modified in some degree by changing the pH of the electrolyte solution. After stabilisation of the flow system, 100 μL aliquotes of 1 M NaCl solutions, buffered at different pH values, were injected directly in the feedstream. (The results for the aminoethanethiol modified surface are available as ESI†.) The larger response

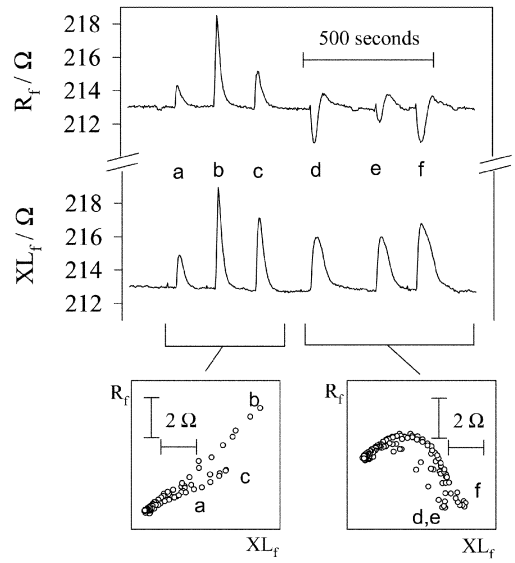

Fig. 3 QCM impedance components R_f and XL_f for 6 injections of different solutions: (a) glycerol 1 M , (b) sucrose 0.25 M, (c) ethyleneglycol 1.6 M, (d) KCl 0.3 M, (e) $CaCl_2$ 0.2 M and (f) $BaCl_2$ 0.3 M. The nonelectrolytes present Kanazawa behaviour, while the electrolytes do not, as can be seen in the corresponding parametric plots (bottom).

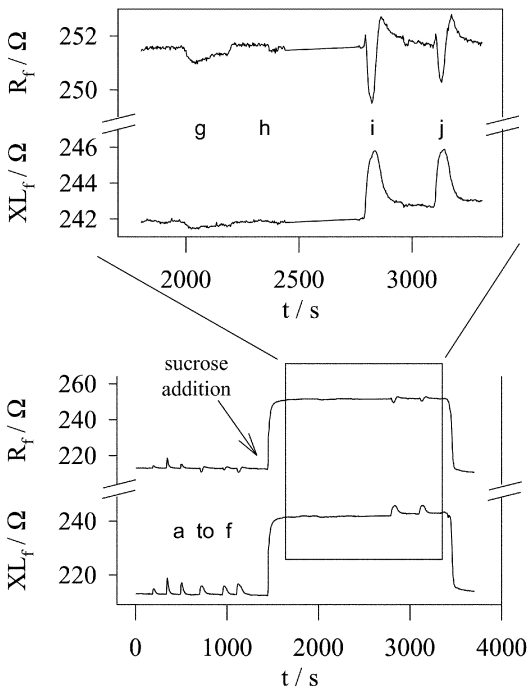

Fig. 4 Complete experiment of which Fig. 3 is the first part (peaks a to f). Bottom: after the six first injections (a to f), sucrose is added to the carrier and the viscosity increases ($t \approx 1500$ s). Top: the enlarged view of the last four injections of (g) glycerol 1 M, (h) sucrose 0.25 M, (i) KCl 0.3 M and (j) NaCl 0.3 M. Note that the QCM response to electrolytes is the same, while the nonelectrolytes do not affect the QCM impedance.

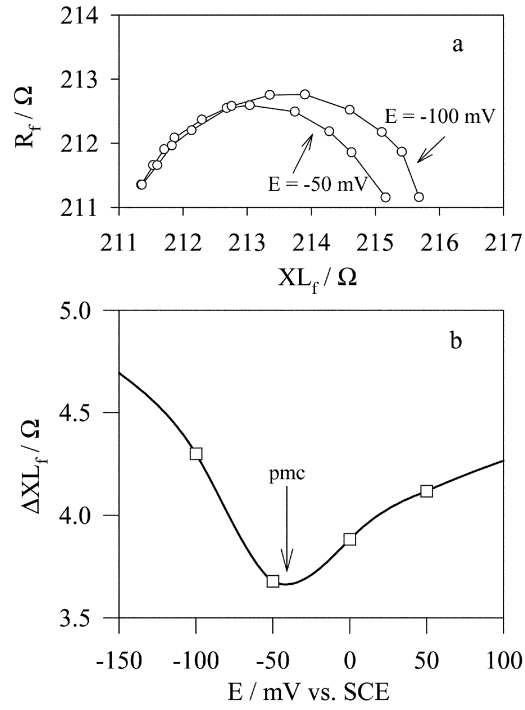

Fig. 5 (a) Parametric polar plots of R_f *vs.* XL_f for two different electrode potentials (quoted *vs.* SCE). [NaCl] increases clockwise from 0 to 6 mM. The open circle for $E = -100$ mV is larger and corresponds to higher moduli and density. (b) Variation of the diameter of the open circles for potentials of −100, −50, 0 and 50 mV. The minimum corresponds to the potential of minimum charge.

corresponds to the injections at lower pH. This tendence is consistent with the presence of $-NH_2$ groups that are charged at low pH. Note that the variation is smooth and there is no evidence of a pK_a of the modified surface. This effect can be due to the fact that on the surface the $-NH_2$ groups are very close, resembling the behaviour of polyaminoelectrolytes (*i.e.* polyallylamine) which present smooth titration curves.[21] For mercaptopropanesulfonate (not shown), the results are qualitatively similar, but in this case the larger semicircles correspond to higher pH. The trends for the semicircle diameter as a function of the pH for both derivatized crystals are shown in Fig. 6.

Fig. 7 shows the parametric plot for the injection of 1 M NaCl at pH = 5.0 over the aminoethanethiol modified gold surface. Note that the parametric curve presents a pronounced hysteresis. Apparently, the fast change in concentration keeps the system away from its equilibrium position indicating that the processes involved may take tens of seconds to equilibrate (the rate of measurement is 1 point per 3 s). Since nonelectrolyte solutions did not show hysteresis at all, this effect cannot be due to any mixing process. Thus, hysteresis can be explained by a slow recovery of the ionic atmosphere when the concentration changes suddenly.

An independent confirmation of the electrostatic nature of this effect can be obtained by comparing the behaviour of the same electrolyte in different solvents. Fig. 8a shows the dependence of both parameters XL_f and R_f as a function of the concentration of tetraethylammonium chloride (TEACl) in water. The plots are very similar to that for the other electrolytes, as can be seen in Fig. 2 and in the ESI.†

Fig. 8b shows the same experiment, but using methanol instead of water. It is evident that the same effect in XL_f and R_f is obtained, but at lower salt concentrations. This is consistent with the lower dielectric constant of the solvent (33 for methanol, 80 for water), which cannot shield the charge of the ions as effectively as water does.

It is important to note that the impedance method used measures both the motional and the static arms of the BVD equivalent circuit. From the obtained magnitudes both series and parallel frequencies can be calculated.[10,11] The changes in the parallel resonant frequency are in the order of kHz, in agreement with previous results,[10,11] and can be ascribed mainly to the extra stray capacitance due to the fringing electric field between the upper electrode and the lower electrode pad through the conductive solution.[11] However, in our experiments, the series resonant frequency also varies, accordingly with Ghafouri and Thompson.[12] This change is much smaller

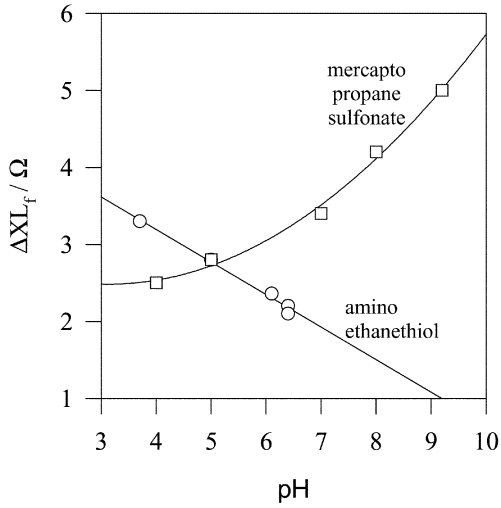

Fig. 6 Dependence of the XL_f responses to pH for injection of NaCl solutions over aminoethanethiol and mercaptopropanesulfonate derivatized gold. Higher surface charge corresponds to higher response of the QCM impedance.

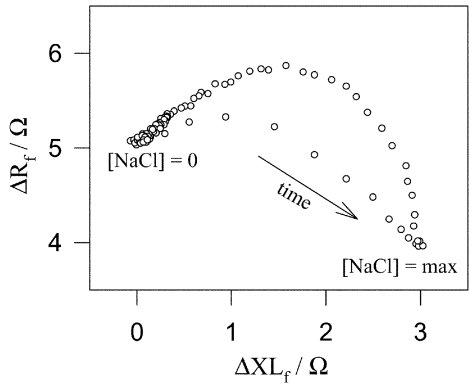

Fig. 7 Parametric plot of R_f *vs.* XL_f for the injection of NaCl. Concentration increases clockwise. Note the hysteresis related with the fast change in concentration at the beginning of the injection.

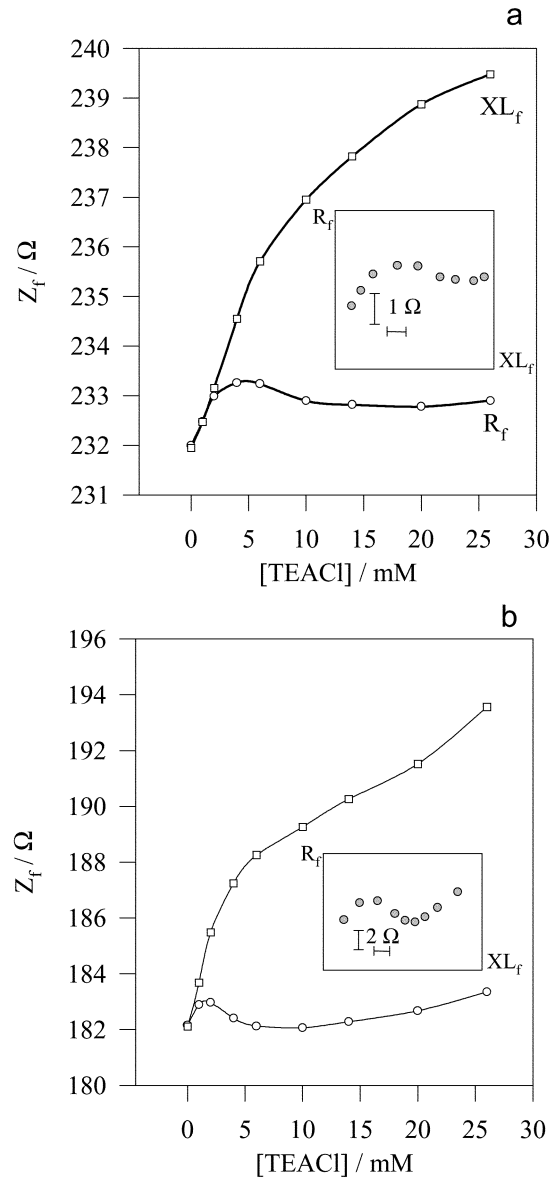

Fig. 8 (a) QCM impedance components R_f and XL_f *vs.* TEACl concentration in water. Each point is the mean value of 10 measurements. Inset: parametric plot of R_f *vs.* XL_f, [TEACl] is the parameter and increases clockwise. (b) The same plot for TEACl in methanol. Note that impedance scales in (a) and (b) are different.

that the former (tens of Hz, corresponding to several ohms in L_f) and cannot be due to the changes in parasitic capacitance. In order to establish the origin of this change, a crystal with one surface completely covered by gold was used to block any electric field reaching the electrolyte solution. This surface was the one in contact with the liquid. In this case, the effect vanishes, showing that the electric field outside of the border of the upper electrode plays an important role in the anomalous behaviour. The acoustoelectric effect,[10,12] produced in the vicinity of the electrode edge, could induce charges on the gold surface which cause the movement of ions on the DDL. In the case of the shielded electrode, the initial movement of the charges due to the acoustoelectric effect does not take place, and the effect is not apparent.

Once the formation of the DDL is proposed as being responsible for the finite viscoelastic film found in the electrolyte solutions, it would be important to estimate some of its rheological properties. In a piezoelectric device, any change in the electric field in the surface of the quartz corresponds to a mechanical motion and vice-versa and therefore mechanical and electrical treatments are equivalent. Mechanical moduli of the electrolyte solution and of the DDL are a consequence of the electric attraction and repulsion between the ions, the thermal agitation and the viscous properties of the solvent. To make the calculations, one needs to take into account that the properties of the layer vary with the distance from the electrode. For regions far away from the crystal, the properties tend to be those of the bulk solution. For small distances, the concentration of ions can change dramatically, depending on the charge of the surface.[16] The characteristic length in which these changes take place is usually referred to as the Debye length d_D. For the studied concentrations, d_D is in the nanometer range. We have assumed that the density ρ, the loss modulus G'' and the elastic modulus G' of the DDL vary exponentially with the distance to the surface d, having the values for the bulk solution at $d \rightarrow \infty$ and maximum values ρ_{max}, G''_{max} and G'_{max} at $d = 0$, as described by eqns. (2)–(4).

$$\rho(d) = \rho_{bulk} + (\rho_{max} - \rho_{bulk})\exp(-d/d_D) \quad (2)$$

$$G''(d) = G''_{bulk} + (G''_{max} - G''_{bulk})\exp(-d/d_D) \quad (3)$$

$$G'(d) = G'_{max}\exp(-d/d_D) \quad (4)$$

In order to obtain values for ρ_{max}, G''_{max} and G'_{max} , we have to calculate the values that satisfy the experimental data of R_f and XL_f. Given three parameters and only two observables, it has been already demonstrated that there is no unique solution, but a set of infinite solutions: Any attempt to obtain the three values of ρ_{max}, G''_{max} and G'_{max} will yield artifacts.[17] To avoid these artifacts, we obtained the moduli values as floating parameters and we fixed the maximum density ρ_{max} as a function of the loss modulus G''. For this purpose, we used the relationship between ρ and η for bulk NaCl solutions.[18] (Note that this is an approximation, since in the close vicinity of the electrode electroneutrality does not hold.) From this data, the phenomenological function $\rho_{max} = 1.679 - 0.667(G''_{max}/G''_{bulk})^{-1/2}$ was derived. Other functionalities between ρ and G'', and even a fixed density ρ yielded similar results. It should be stressed that these calculations are performed only to estimate orders of magnitude and trends in the viscoelastic behaviour of the DDL, and not to obtain the exact values of the viscoelastic moduli of the layer.

Modeling of the viscoelastic DDL has been performed by using Martin's multilayer model.[12] The DDL was considered to be composed of 99 slices, each one of constant ρ, G'' and G'. The thickness of each layer is $0.03d_D$. In this way, the slices fall in the region closer than $3d_D$ from the quartz surface. After this point, a layer of semi-infinite liquid is considered, with properties $\rho_{bulk} = 1$ g cm^{-3}, $G''_{bulk} = 60$ kPa and $G'_{bulk} = 0$. To calculate the impedance corresponding to a given set of ρ_{max}, G''_{max} and G'_{max} and d_D, the matrix propagation method[12] was employed. For each experimental point, the values that satisfy the R_f and XL_f measurement were found by means of a simplex algorithm and iterated until the error between the experimental data and the model was less than 0.01 Ω, which is less than the experimental error (0.05 Ω).

Fig. 9 shows the results of this calculation, based on the experimental points of Fig. 2. In the upper plot, the loss modulus G''_{max} increases with the concentration, showing that the DDL becomes considerably more viscous as the bulk concentration increases. The DDL viscosity in the vicinity of the electrode at [NaCl] = 40 mM is 2.5 times the viscosity of pure water (η = 2.5 cp) . As a comparison, the maximum possible viscosity of an aqueous NaCl solution is η = 2 cp, corresponding to its saturation concentration of 5.3 M. The DDL also shows elasticity that varies from zero for pure water to 50 kPa for the maximum concentration. The third plot of Fig. 9 shows the density ρ_{max} at the crystal surface. For bulk solutions of NaCl, the density is a linear function of the concentration[18] $\rho = 1 + 0.0376$[NaCl]. Extrapolating this relationship, the concentration for the innermost layer is $[NaCl]_{max} = 6.75$ M. By using the Grahame equation [eqn. (5)] it is possible to estimate the charge on the surface:

$$\sum_i c_{0i} = \sum_i c_{\infty i} + \sigma^2 / 2\varepsilon\varepsilon_0 kT \quad (5)$$

For [NaCl] = 6.75 M, the charge $\sigma = 0.15$ C m^{-2}. This value corresponds approximately to one electronic charge per nm^2.

The fourth plot in Fig. 9 shows the reciprocal of the loss tangent ($\alpha^{-1} = G'_{max}/G''_{max}$) as a function of the concentration. Note that the elastic contribution presents a steep increase between 0 and 10 mM and remains almost constant after this concentration.

While the increase in viscosity can be attributed mainly to the high electrolyte concentration near the surface, the elasticity could be explained in terms of the relaxation of the ionic

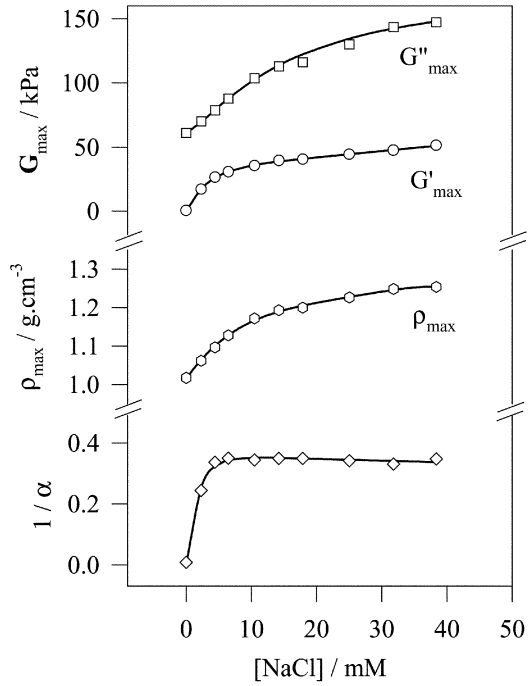

Fig. 9 Estimation of the rheological properties of the diffuse double layer in the innermost region as function of the bulk NaCl concentration. From top to bottom: loss modulus G''_{max}, elastic modulus G'_{max}, solution density ρ_{max} and the reciprocal of the loss tangent $\alpha^{-1} = G'_{max}/G''_{max}$. The values were obtained from data in Fig. 2, by using Martin's multilayer model (see text).

atmosphere. When the charges at the surface oscillates at 10 MHz, the atmosphere cannot follow their fast movement and a restitutive elastic force acts on the surface. A similar phenomena was already observed in bulk solutions of polyelectrolytes.[13]

5. Conclusions

In this work, we have shown that the response of the QCM to solutions of electrolytes shows non-Kanazawa behaviour, that can be explained by means of a finite viscoelastic layer close to the quartz crystal surface. This behaviour does not depend on the chemical nature of the surface, but on its charge, as can be shown from experiments using potential-clamped electrodes and derivatised surfaces. The effect is highly reproducible, and is proved for many electrolytes. This anomaly does not appear if the quartz side in contact with the solution is completely covered with gold, showing that an electric field outside the edge of the electrode plays an important role, probably through the acoustoelectric effect. These results also indicates that the shielding of the entire electrode is a suitable method to minimize the errors in adsorption microgravimetries.

We propose that the above mentioned behaviour is due to the formation of the diffuse electric double layer (DDL), which presents a strong viscoelasticity. The proposed model is in excellent agreement with the experimental data measured for differently charged surfaces in contact with dilute electrolyte solutions varying from 0 to 50 mM. We have demonstrated that the surface charge and the dielectric constant of the solvent play important roles in the viscoelastic properties of this layer. The characteristic times and the hysteresis indicate that this is a long range effect, possibly related to the ionic atmosphere relaxation, and not simply a surface process. The ionic atmosphere cannot follow the surface movement at 10 MHz, and this may explain the observed elasticity. To model the mechanical elasticity of the DDL, further investigations are being carried out.

Acknowledgements

Fruitful discussions with Dr David Soares are acknowledged. This work was supported by Fundacion Antorchas and PROMEP.

References

1 P. Delahay, in *Double Layer and Electrode Kinetics, Part I*, Interscience, New York, 1965.
2 R. E. White, in *Modern Aspects of Electrochemistry no. 22*, Plenum Press, New York, 1992.
3 T. Mattke and H. J. Kecke, *J. Colloid Interface Sci.*, 1998, **208**, 555.
4 A. C. Hillier, S. Kim and A. J. Bard, *J. Phys. Chem.*, 1996, **100**, 18808.
5 M. A. Noel and P. A. Topart, *Anal. Chem.*, 1994, **66**, 484.
6 H. Muramatsu and K. Kimura, *Anal. Chem.*, 1992, **64**, 2502.
7 R. A. Etchenique and E. J. Calvo, *Anal. Chem.*, 1997, **69**(23), 4833.
8 R. Lucklum and P. Hauptmann, *Faraday Discuss.*, 1997, **107**, 123.
9 R. Etchenique and T. Buhse, *Analyst*, 2000, **125**, 785.
10 Z. A. Shana and F. Josse, *Anal. Chem.*, 1994, **66**, 1955–1964.
11 M. Rodahl, F. Hook and B. Kasemo, *Anal. Chem.*, 1996, **68**, 2219–2227.
12 S. Ghafouri and M. Thompson, *Analyst*, 2001, **126**, 2159–2167.
13 E. J. Calvo, R. Etchenique, P. N. Bartlett, K. Singhal and C. Santamaria, *Faraday Discuss.*, 1997, **107**, 141.
14 R. A. Etchenique and E. J. Calvo, *Electrochem. Commun.*, 1999, **1**(5), 167.
15 P. A. Topart and M. A. Noël, *Anal. Chem.*, 1994, **66**, 2926.
16 J. N. Israelachvili, *Intermolecular and Surface Forces*, Academic Press, London, 2nd edn., 1991.
17 R. Etchenique and A. D. Weisz, *J. Appl. Phys.*, 1999, **86**, 1994.
18 *CRC Handbook of Chemistry and Physics*, ed. R. C. Weast, The Chemical Rubber Company, Ohio, 53rd edn., 1972.
19 M. Stratmann and V. Tsionsky, *Faraday Discuss.*, 1997, **107**, 382.
20 R. Etchenique, M. Furman and J. Olabe, *J. Am. Chem. Soc.*, 2000, **122**(16), 3967.
21 Y. Yoshikawa, H. Matsuoka and N. Ise, *Br. Polym. J.*, 1986, **18**(4), 242.